Soliton localization in Bose–Einstein condensates with time-dependent harmonic potential and scattering length

Soliton localization in Bose–Einstein condensates with time-dependent harmonic potential and scattering length

U Al Khawaja

Physics Department, United Arab Emirates University, PO Box 17551, Al-Ain, United Arab Emirates

Abstract
We derive exact solitonic solutions of a class of Gross–Pitaevskii equations with a time-dependent harmonic trapping potential and interatomic interaction. We find families of exact single-solitonic, multi-solitonic and solitary wave solutions. We show that, with the special case of an oscillating trapping potential and interatomic interaction, a soliton can be localized indefinitely at an arbitrary position. The localization is shown to be experimentally possible for sufficiently long time even with only an oscillating trapping potential and a constant interatomic interaction.

PACS numbers: 02.30.Ik, 02.30.Jr, 05.45.Yv

(Some figures in this article are in colour only in the electronic version)

1. Introduction

The experimental realization of solitons in Bose–Einstein condensates [1–6] has stimulated intense interest in their properties [7–15]. The inhomogeneity provided by the trapping potential has renewed the old [16–20] and more recent [21] interest in the different aspects of one- and multi-soliton dynamics in inhomogeneous potentials.

In the experiments of [5, 4], stable bright solitons were created and set in a particle-like center-of-mass motion. The wave nature of solitons was revealed when two adjacent solitons repelled each other as a result of their phase difference [9]. On the other hand, it is established that bright solitons collapse when the number of atoms exceeds a certain limit [22]. This results from the attractive Hartree energy overcoming the repulsive kinetic energy pressure. One of the methods proposed to stabilize the soliton against collapsing is to rapidly oscillate the interatomic interaction or the trapping potential [23]. Obviously, the inhomogeneity imposed by the trapping potential plays an important role on the dynamics and stability of solitons.

The evolution of solitons is approximately described by the inhomogeneous nonlinear Schrödinger equation known as the Gross–Pitaeviskii equation [24, 25]. The approximation stems from the fact that the Gross–Pitaevskii equation is a mean-field approximation of the exact N-particle Schrödinger equation. While in some cases the soliton dynamics obtained by these two equations disagree [26], the Gross–Pitaevskii equation often gives accurate results. Theoretical studies performed to account for the observed behavior of solitons were conducted by solving the Gross–Pitaevskii equation with numerical, perturbative or variational methods. Much less effort was devoted to finding exact solutions of this equation [18, 27–34]. In addition to providing rigorous insight, exact solutions acquire valuable importance when problems such as soliton–soliton collisions and soliton interaction with potentials are addressed. In such cases, formulae for the force between solitons or soliton's effective mass can be derived [35]. In addition, obtaining such exact solutions allows for testing the validity of the Gross–Pitaevskii equation at high soliton densities and obtaining the long-time evolution of the soliton where numerical techniques aught to break down.

Here, we further explore exact solitonic solutions of the Gross–Pitaevskii equation. Specifically, the goal of this paper is two-fold. First, we investigate the existence and properties of solitonic solutions in the presence of a time-dependent trapping potential and interatomic interaction. Second, we focus on the effect of an oscillating trapping potential and interatomic interaction on the center-of-mass motion of the soliton. We consider here only the case of attractive interatomic interactions which allows for bright solitons.

The first goal is achieved by employing the Darboux transformation method [36] to derive families of exact solitonic solutions of a class of Gross–Pitaevskii equations. It should be noted that the main solution we derive here (equation (22)), which corresponds to a harmonic expulsive potential, reproduces a special case of the general solution found by Serkin *et al* corresponding to a combination of a harmonic and linear potentials [21]. Hence, the significance of the first goal is mainly presenting a systematic method of generating exact solutions.

For the second goal, we considered the special case of oscillating strengths of the harmonic trapping potential and interatomic interaction. Interestingly enough, it turns out that such oscillations not only stabilize the soliton against shrinking, but also make it possible to localize it at an arbitrary position. This is the main result of this paper. The possibility of localizing the soliton is then discussed from an experimental point of view. To that end, we considered the nonintegrable, though experimentally simpler, case of only an oscillating trapping potential and constant interatomic interaction. Here too, the soliton can be localized, though not indefinitely as before. The long-time evolution shows that the soliton continues to be trapped but will be oscillating around the minimum of the harmonic potential. For a typical experimental setup, we show that the soliton can be localized around its initial position for a time period of the order of, or even larger than, the lifetime of the soliton. The soliton localization suggests a management mechanism for the soliton position and speed that may have applications in various situations such as soliton–soliton collisions and soliton interaction with potentials.

The rest of the paper is organized as follows. In the following section, we present the general form of the Gross–Pitaevskii equation to be solved. In section 3, we use the Darboux transformation method to derive the new solitonic solutions. We then discuss their properties, dynamics and localization. In section 4, we discuss the experimental feasibility of realizing soliton localization. We end in section 5 with a summary of our main results and conclusions.

2. The Gross–Pitaevskii equation

The Gross–Pitaevskii equation describing a Bose–Einstein condensate trapped by an axially symmetric harmonic potential with attractive interatomic interactions is given by

$$i\hbar \frac{\partial}{\partial t}\psi(\mathbf{r}, t) = \left[-\frac{\hbar^2}{2m}\nabla_{\mathbf{r}}^2 + \frac{1}{2}m\left(\omega_x^2 x^2 + \omega_\perp^2 (y^2 + z^2)\right) - \frac{4\pi a_s \hbar^2}{m}|\psi(\mathbf{r}, t)|^2 \right]\psi(\mathbf{r}, t), \qquad (1)$$

where a_s is the absolute value of the s-wave scattering length, and ω_x and $\omega_\perp$ are the characteristic frequencies of the harmonic trapping potential in the axial and radial directions, respectively.

When the confinement of the Bose–Einstein condensate is much larger in the y- and z-directions compared to the confinement in the x-direction, the system can be considered effectively one-dimensional along the x-direction. The three-dimensional Gross–Pitaevskii equation can then be *integrated* over the y- and z-directions to result in a one-dimensional Gross–Pitaevskii equation [7, 37]

$$i\hbar \frac{\partial}{\partial t}\psi(x, t) = \left[-\frac{\hbar^2}{2m}\frac{\partial^2}{\partial x^2} + \frac{1}{2}m\omega_x^2 x^2 - 2\lambda a_s|\psi(x, t)|^2 \right]\psi(x, t), \qquad (2)$$

where $\lambda = \omega_\perp/\omega_x$. Scaling length to $a_x = \sqrt{\hbar/m\omega_x}$, time to $1/\omega_x$, and $\psi(x, t)$ to $1/\sqrt{2\lambda a_x}$, the Gross–Pitaevskii equation takes the dimensionless form

$$i\frac{\partial}{\partial t}\psi(x, t) = \left[-\frac{1}{2}\frac{\partial^2}{\partial x^2} + \frac{1}{2}p(t)x^2 - aq(t)|\psi(x, t)|^2 \right]\psi(x, t), \qquad (3)$$

where $a = a_s/a_x$ is the scaled scattering length. The dimensionless general functions $p(t)$ and $q(t)$ are introduced to account for the time dependencies of the strengths of the trapping potential and the interatomic interaction.

In the following section, it is shown that this equation is integrable only if $p(t)$ and $q(t)$ are parametrically related as follows: $p(t) = \ddot{\gamma}(t) - \dot{\gamma}(t)^2$ and $q(t) = \exp(\gamma(t))$, where $\gamma(t)$ is an arbitrary real function (see equation (7)). We find exact solitonic solutions of equation (3) below in terms of the function $\gamma(t)$. A host of rich and interesting physical systems are described by such a class of solutions. In particular, an oscillating form of $\gamma(t)$ will be considered in this paper.

3. Darboux transformation and the exact solutions

3.1. Darboux transformation

Applying the Darboux transformation method on nonlinear partial differential equations requires finding a linear system of equations for an *auxiliary* field $\Psi(x, t)$. The linear system is usually written in a compact form in terms of a pair of matrices as follows: $\Psi_x = \mathbf{U} \cdot \Psi$ and $\Psi_t = \mathbf{V} \cdot \Psi$. The matrices $\mathbf{U}$ and $\mathbf{V}$, known as the Lax pair, are functionals of the solution of the differential equation. The *consistency condition* of the linear system $\Psi_{xt} = \Psi_{tx}$ is required to be equivalent to the partial differential equation under consideration. Applying the Darboux transformation, as defined below, on Ψ transforms it into another field $\Psi[1]$. For the transformed field $\Psi[1]$ to be a solution of the linear system, the Lax pair must also be transformed in a certain manner. The transformed Lax pair will be a functional of a new solution of the same differential equation.

Practically, this is performed as follows. First, we find the Lax pair and an exact solution of the differential equation, known as the *seed* solution. Fortunately, the trivial solution can be used as a seed, leading to nontrivial solutions. Using the Lax pair and the seed solution, the

linear system is then solved and the components of $\boldsymbol{\Psi}$ are found. The new solution is expressed in terms of these components and the seed solution. The following detailed derivation of the new solution clarifies this procedure further.

Using our Lax pair search method [38], we find the following linear system which corresponds to the class of Gross–Pitaevskii equations we are interested in:

$$\boldsymbol{\Psi}_x = \zeta \mathbf{J} \cdot \boldsymbol{\Psi} \cdot \Lambda + \mathbf{U} \cdot \boldsymbol{\Psi}, \tag{4}$$

$$\boldsymbol{\Psi}_t = i\zeta^2 \mathbf{J} \cdot \boldsymbol{\Psi} \cdot \Lambda \cdot \Lambda + \zeta \left(i\mathbf{U} + x\gamma(t)\mathbf{J} \right) \cdot \boldsymbol{\Psi} \cdot \Lambda + \mathbf{V} \cdot \boldsymbol{\Psi}, \tag{5}$$

where

$$\boldsymbol{\Psi}(x,t) = \begin{pmatrix} \psi_1(x,t) & \psi_2(x,t) \\ \phi_1(x,t) & \phi_2(x,t) \end{pmatrix}, \qquad \mathbf{J} = \begin{pmatrix} 1 & 0 \\ 0 & -1 \end{pmatrix},$$

$$\Lambda = \begin{pmatrix} \lambda_1 & 0 \\ 0 & \lambda_2 \end{pmatrix}, \qquad \mathbf{U} = \begin{pmatrix} 0 & \sqrt{a}\,Q(x,t) \\ -\sqrt{a}\,Q^*(x,t) & 0 \end{pmatrix},$$

$$\mathbf{V} = \begin{pmatrix} ia|Q(x,t)|^2/2 & \sqrt{a}\lambda x\dot{\gamma}\,Q(x,t) + i\sqrt{a}\,Q_x(x,t)/2 \\ -\sqrt{a}\lambda x\dot{\gamma}\,Q^*(x,t) + i\sqrt{a}\,Q_x^*(x,t)/2 & -ia|Q(x,t)|^2/2 \end{pmatrix},$$

$\zeta(t) = \exp(\gamma(t))$, and λ_1 and λ_2 are arbitrary constants. For convenience, we presented the matrices in terms of the function $Q(x,t)$ which is related to the wavefunction as follows $Q(x,t) = \psi(x,t)e^{(\gamma(t)+i\dot{\gamma}(t)x^2)/2}$.

It should be emphasized that while applying the Darboux transformation is almost straightforward, finding a linear system that corresponds to the differential equation at hand is certainly not a trivial matter. Usually, this is found by trial and error, or by starting from a certain linear system and then finding the differential equation it corresponds to. In [38], we have introduced a systematic approach to find the linear system which we describe here briefly. The partial derivatives of the auxiliary field, $\boldsymbol{\Psi}_x$ and $\boldsymbol{\Psi}_t$, are expanded in powers of Λ with unknown matrix coefficients. The expansions are terminated at the first order for $\boldsymbol{\Psi}_x$ and the second order for $\boldsymbol{\Psi}_t$ since this will be sufficient to generate the class of Gross–Pitaevskii equations under consideration. The higher order matrix coefficients turn out to be essentially determined by the zeroth-order matrix coefficients $\mathbf{U}$ and $\mathbf{V}$. To find the matrices $\mathbf{U}$ and $\mathbf{V}$, we expand them in powers of the wavefunction $\psi(x,t)$, its complex conjugate, and their partial derivatives. The coefficients of the expansions are unknown functions of x and t. Substituting these expansions in the consistency condition (equation (6) below) we find a set of equations for the unknown function coefficients. Finally, by solving these equations the Lax pair and consequently the linear system will be determined. The linear system found here is a generalization to that of Zakharov–Shabat for homogeneous Gross–Pitaevskii equation [39].

For $\boldsymbol{\Psi}$ to be a solution of both equations (4) and (5), the consistency condition $\boldsymbol{\Psi}_{xt} = \boldsymbol{\Psi}_{tx}$ must be satisfied. This condition leads to the following relation between the matrices $\mathbf{U}$ and $\mathbf{V}$:

$$\mathbf{U}_t - \mathbf{V}_x + [\mathbf{U}, \mathbf{V}] = 0, \tag{6}$$

where $[\mathbf{U}, \mathbf{V}]$ is the commutator of $\mathbf{U}$ and $\mathbf{V}$. Substituting the above expressions for $\mathbf{U}$ and $\mathbf{V}$ in the last equation, we obtain the Gross–Pitaevskii equation

$$i\frac{\partial}{\partial t}\psi(x,t) = \left[-\frac{1}{2}\frac{\partial^2}{\partial x^2} + \frac{1}{2}\left(\ddot{\gamma}(t) - \dot{\gamma}(t)^2 \right) x^2 \psi(x,t) - ae^{\gamma(t)}|\psi(x,t)|^2 \right] \psi(x,t), \tag{7}$$

and its complex conjugate. This equation shows that the functions $p(t)$ and $q(t)$ are parametrically related to each other through the general function $\gamma(t)$. In [21], Serkin *et al*

solve a nonautonomous Gross–Pitaevskii equation that is similar to equation (7) but with additional time-dependent dispersion and linear potential. Similar to our conclusion [38], the authors of this reference and [34] found that relations between the coefficients must be obeyed for the model to be integrable. We focus here on the specific case of only a harmonic trapping potential and constant dispersion. The linear system of eight equations, equations (4) and (5), read explicitly

$$\psi_{1x} - \phi_1 \sqrt{a} e^{\frac{1}{2}(i\dot{\gamma}x^2+\gamma)}\psi_0 - \sqrt{2}\lambda_1\psi_1 e^{\gamma} = 0, \tag{8}$$

$$\psi_{2x} - \phi_2 \sqrt{a} e^{\frac{1}{2}(i\dot{\gamma}x^2+\gamma)}\psi_0 - \sqrt{2}\lambda_2\psi_2 e^{\gamma} = 0, \tag{9}$$

$$\phi_{1x} + \sqrt{2}\lambda_1 e^{\gamma}\phi_1 + \psi_0^*\psi_1\sqrt{a}e^{\frac{1}{2}(\gamma-ix^2\dot{\gamma})} = 0, \tag{10}$$

$$\phi_{2x} + \sqrt{2}\lambda_2 e^{\gamma}\phi_2 + \psi_0^*\psi_2\sqrt{a}e^{\frac{1}{2}(\gamma-ix^2\dot{\gamma})} = 0, \tag{11}$$

$$\psi_{1t} - i\psi_1 e^{\gamma}\left(2e^{\gamma}\lambda_1^2 - i\sqrt{2}x\dot{\gamma}\lambda_1 + \frac{1}{2}|\psi_0|^2 a\right)$$
$$- \frac{1}{2}\phi_1\sqrt{a}e^{\frac{1}{2}(i\dot{\gamma}x^2+\gamma)}\left(i\psi_{0x} + \psi_0\left(2i\sqrt{2}e^{\gamma}\lambda_1 + x\dot{\gamma}\right)\right) = 0, \tag{12}$$

$$\psi_{2t} - i\psi_2 e^{\gamma}\left(2e^{\gamma}\lambda_2^2 - i\sqrt{2}x\dot{\gamma}\lambda_2 + \frac{1}{2}|\psi_0|^2 a\right)$$
$$- \frac{1}{2}\phi_2\sqrt{a}e^{\frac{1}{2}(i\dot{\gamma}x^2+\gamma)}\left(i\psi_{0x} + \psi_0\left(2i\sqrt{2}e^{\gamma}\lambda_2 + x\dot{\gamma}\right)\right) = 0, \tag{13}$$

$$\phi_{1t} + \frac{1}{2}\psi_1\sqrt{a}e^{\frac{1}{2}(\gamma-ix^2\dot{\gamma})}\left(\psi_0^*\left(2i\sqrt{2}e^{\gamma}\lambda_1 + x\dot{\gamma}\right) - i\psi_{0x}^*\right)$$
$$+ \frac{1}{2}\phi_1 e^{\gamma}\left(i|\psi_0|^2 a + 2\lambda_1\left(2ie^{\gamma}\lambda_1 + \sqrt{2}x\dot{\gamma}\right)\right) = 0, \tag{14}$$

$$\phi_{2t} + \frac{1}{2}\psi_2\sqrt{a}e^{\frac{1}{2}(\gamma-ix^2\dot{\gamma})}\left(\psi_0^*\left(2i\sqrt{2}e^{\gamma}\lambda_2 + x\dot{\gamma}\right) - i\psi_{0x}^*\right)$$
$$+ \frac{1}{2}\phi_2 e^{\gamma}\left(i|\psi_0|^2 a + 2\lambda_2\left(2ie^{\gamma}\lambda_2 + \sqrt{2}x\dot{\gamma}\right)\right) = 0, \tag{15}$$

where $\psi_0(x,t)$ is an exact seed solution of equation (7). These equations reduce to an equivalent system of four equations with nontrivial solutions by making the following substitutions: $\lambda_1 = -\lambda_2^*$, $\psi_2 = \phi_1^*$ and $\phi_2 = -\psi_1^*$. Using the trivial solution, $\psi_0(x,t) = 0$, as a seed, the linear system will have the solution

$$\psi_1(x,t) = c_1 e^{2i\lambda_1^2\int e^{2\gamma(t)}dt + e^{\gamma(t)}\lambda_1 x}, \tag{16}$$

$$\phi_2(x,t) = c_2 e^{-2i\lambda_1^2\int e^{2\gamma(t)}dt - e^{\gamma(t)}\lambda_1 x}, \tag{17}$$

where c_1 and c_2 are real arbitrary constants of integration.

Consider the following version of the Darboux transformation [36]:

$$\Psi[1] = \Psi \cdot \Lambda - \sigma\Psi, \tag{18}$$

where $\Psi[1]$ is the transformed field, $\sigma = \Psi_0 \cdot \Lambda \cdot \Psi_0^{-1}$. Here Ψ_0 is a known (seed) solution of the linear system equations (8)–(15). For the transformed field $\Psi[1]$ to be a solution of the linear system, the matrix **U** for instance must be transformed as[1]

$$\mathbf{U}[1] = \sigma \cdot \mathbf{U} \cdot \sigma^{-1} + \sigma_x \cdot \sigma^{-1}, \tag{19}$$

---

[1] Since the new solution can already be extracted from equation (19), there is no need to write the more complicated equation for **V**[1] which leads to the same result.

where σ^{-1} is the inverse of σ. This equation gives the new solution in terms of the seed solutions of the Gross–Pitaevskii equation, $\psi_0(x, t)$, and the linear system, Ψ_0, which reads

$$\psi(x, t) = \psi_0(x, t) + \frac{2}{a}(\lambda_1 + \lambda_1^*)e^{-i\dot{\gamma}(t)x^2/4+\gamma(t)/2}\frac{\phi_1\psi_1^*}{|\phi_1|^2 + |\psi_1|^2}. \tag{20}$$

3.2. Exact single-solitonic solution

Using $\psi_0(x, t) = 0$ and equations (16) and (17), the new solution takes the form

$$\psi(x, t) = \frac{4\sqrt{2}\lambda_{1r}c_1c_2{}^*}{\sqrt{a}}\frac{e^{\gamma(t)/2+i\theta(t)}}{|c_1|^2e^{\beta(t)x-x_0(t)} + |c_2|^2e^{-(\beta(t)x-x_0(t))}}, \tag{21}$$

where $\theta(t) = -4(\lambda_{1i}{}^2 - \lambda_{1r}{}^2)\int e^{2\gamma(t)}dt + x(2e^{\gamma(t)}\lambda_{1i} - x\dot{\gamma}(t)/\sqrt{8})$, $\beta(t) = 2\sqrt{2}\lambda_{1r}e^{\gamma(t)}$, and $x_0(t) = 8\lambda_{1i}\lambda_{1r}\int e^{2\gamma(t)}dt$. Here c_1, c_2, λ_1 and λ_2 are arbitrary constants. The subscripts r and i denote real and imaginary parts, respectively. Substituting $c_1 = \exp(\delta_1)$, $c_2 = \exp(\delta_2)$, where δ_1 and δ_2 are arbitrary constants, completing the square in the phase factor, and normalizing $\psi(z, t)$ to N, this solution can be recast in the following more appealing form:

$$\psi(x, t) = \frac{\sqrt{N}\sqrt{Na}}{2}e^{\gamma(t)/2+i\phi(x,t)}\text{sech}\left(\frac{Na}{2}e^{\gamma(t)}(x - x_{cm}(t))\right), \tag{22}$$

where

$$\phi(x, t) = \phi_0(t) + \dot{x}_{cm}(t)(x - x_{cm}(t)) - \frac{1}{2}\dot{\gamma}(t)(x - x_{cm}(t))^2, \tag{23}$$

$$x_{cm}(t) = \left(x_0 e^{2\gamma(0)} + (v_0 + x_0\dot{\gamma}(0))g(t)\right)e^{-\gamma(t)-\gamma(0)}, \tag{24}$$

$$\phi_0 = c_3 - \frac{1}{2}\dot{\gamma}(t)^2 x_{cm}(t)^2 + \frac{1}{2}\left(\frac{1}{4}(aN)^2 + e^{-2\gamma(0)}(v_0 + x_0\dot{\gamma}(0))^2\right)g(t), \tag{25}$$

$g(t) = \int_0^t e^{2\gamma(t')}dt'$. The constant c_3 corresponds to an arbitrary overall phase.

This solution corresponds to a sech-shaped soliton containing N atoms with a time-dependent center of mass $x_{cm}(t)$ and time-dependent width $2\exp(-\gamma t)/Na$. The linear part of the phase profile shows that the soliton is moving with a center-of-mass velocity $v(t) = \dot{x}_{cm}(t)$. The quadratic part corresponds to a phase chirp associated with the quadratic trapping potential.

The simple choice $\gamma(t) = $ constant, which corresponds to the homogeneous Gross–Pitaevskii equation, gives $x_{cm}(t) = v_0 t + x_0$. The solitonic solution in this case corresponds to the well-known sech-shaped soliton with a center-of-mass moving with a constant velocity v_0 and starting the motion at the initial position x_0. In the limit $\gamma(t) \to 0$, the solution, equation (22), reduces to

$$\psi(x, t) = \frac{\sqrt{N}\sqrt{Na}}{2}e^{i\phi(t)}\text{sech}\left(\frac{Na}{2}(x - (x_0 + v_0 t))\right), \tag{26}$$

where $\phi(t) = c_3 + ((aN)^2 + 4v_0^2)t/8 + v_0(x - (x_0 + v_0 t))$. This is the well-known sech solution of the homogeneous Gross–Pitaevskii equation. For $\gamma(t) = $ constant $\times t$ we get a Gross–Pitaevskii equation with an expulsive harmonic potential and exponentially growing interatomic interaction [30]. In principle, we can choose any form of $\gamma(t)$, but one should keep in mind that the interatomic interaction strength is proportional to $\exp(\gamma(t))$. Such a time dependence may not be realistic from an experimental point of view for any $\gamma(t)$.

In [21] Serkin *et al* have already derived the exact solitonic solution of a Gross–Pitaevskii equation with a linear and quadratic potentials and time-dependent dispersion

$$i\frac{\partial}{\partial t}\psi(x,t) = \left[-\frac{D(t)}{2}\frac{\partial^2}{\partial x^2} - \frac{\Omega^2(t)}{2}x^2 - 2\alpha(t)x - aR(t)|\psi(x,t)|^2\right]\psi(x,t). \tag{27}$$

The authors show that this equation is integrable only if the functions $D(t)$, $\Omega(t)$ and $R(t)$ are related to each other through the *integrability condition* (equation (2) in [21]). The special case of only a quadratic potential and constant dispersion corresponds to the Gross–Pitaevskii equation considered in this paper. Substituting $\alpha(t) = 0$ and $D(t) = 1$ in equation (2) of [21], the integrability condition simplifies to $\Omega^2 = -\dot{\gamma}^2 + \ddot{\gamma}$, which shows that, in this special case, the previous equation is indeed equivalent to equation (7). Therefore, substituting $\alpha(t) = 0$ and $D(t) = 1$ in the general solution of equation (27), namely equation (8) in [21], should result in our solution, equation (22). It turns out, however, that the two solutions do not match exactly. The solution of [21] corresponds to a soliton located initially at $x = 0$ while in our case the soliton is located initially at the arbitrary position x_0. This can be clearly seen by substituting, without loss of generality, $\eta(t) = Na\exp(\gamma(t))/4$ and $\kappa(t) = -v_0\exp(-\gamma(0))/2$ in the argument of the sech function of equation (8) of [21]. This results in a center-of-mass coordinate $x_{cm}(t) = v_0 g(t)e^{-\gamma(t)-\gamma(0)}$. Since $g(0) = 0$, this shows that $x_{cm}(0) = 0$ in contrast with our case $x_{cm}(0) = x_0$.

The dynamics of the soliton is readily given by equation (24). An equation of motion for the center of mass $x_{cm}(t)$ can be derived from the Euler's equation of the Lagrangian $L[x_{cm}, \dot{x}_{cm}] = \int_{-\infty}^{\infty} i dx \psi^* \partial\psi/\partial t - E[x_{cm}, \dot{x}_{cm}]$. The energy functional is given by

$$E[x_{cm}, \dot{x}_{cm}]$$
$$= \int_{-\infty}^{\infty} \psi^*(x,t)\left[-\frac{1}{2}\frac{\partial^2}{\partial x^2} + \frac{1}{2}(\ddot{\gamma}(t) - \dot{\gamma}(t)^2)x^2 - \frac{1}{2}ae^{\gamma(t)}|\psi(x,t)|^2\right]\psi(x,t), \tag{28}$$

which results in the equation of motion

$$\ddot{x}_{cm}(t) + (\ddot{\gamma} - \dot{\gamma}^2)x_{cm}(t) = 0. \tag{29}$$

This equation shows that the center-of-mass motion is determined by the function $\gamma(t)$. Thus, interatomic interactions do not affect the center-of-mass motion which is a manifestation of Kohn's theorem [40].

3.3. Oscillating trapping potential

In this section, we consider an oscillating form of $\gamma(t)$ which results in a trapping potential and interatomic interaction with oscillating strengths. A first simple choice for $\gamma(t)$ would be for instance $\cos(\omega t + \delta)$. However, in this case, the interatomic interaction, which will be proportional to $\exp(\cos\omega t + \delta)$, oscillates nonlinearly. Such a time-dependent interatomic interaction may not be possible to realize experimentally. Instead, we use the form

$$\gamma(t) = \frac{1}{2}(\alpha_1 + \alpha_2\cos(\omega t + \delta)), \tag{30}$$

where $\alpha_1, \alpha_2, \omega$ and δ are arbitrary dimensionless constants. In this case, the Gross–Pitaevskii equation, equation (7), takes the form

$$i\frac{\partial\psi(x,t)}{\partial t} = \left[-\frac{1}{2}\frac{\partial^2}{\partial x^2} - \frac{1}{4}\alpha_2\omega^2\left(\cos(\omega t + \delta) + \frac{1}{2}\alpha_2\sin(\omega t + \delta)^2\right)x^2 \right.$$
$$\left. - ae^{(\alpha_1 + \alpha_2\cos(\omega t + \delta))/2}|\psi(x,t)|^2\right]\psi(x,t). \tag{31}$$

The advantage of this particular form of $\gamma(t)$ is that, for $\alpha_2 \ll 1$, the amplitude of the oscillation in the interatomic interaction can be set to an arbitrarily small value such that the strength of the interatomic interaction can be considered practically as constant. Substituting this expression for $\gamma(t)$ in equation (29), we get

$$\ddot{x}_{\text{cm}} - \frac{1}{4}\alpha_2\omega^2 \left(2\cos\left(\omega t + \delta\right) + \alpha_2 \sin\left(\omega t + \delta\right)^2\right) x_{\text{cm}} = 0. \tag{32}$$

The general solution of this equation is readily given by equation (24), which now takes the form

$$x_{\text{cm}}(t) = x_0 e^{\frac{\alpha_2}{2}(\cos\delta - \cos(\omega t + \delta))} + \left(v_0 - \frac{1}{2}x_0\alpha_2\omega\sin\delta\right) e^{-\frac{\alpha_2}{2}(\cos\delta + \cos(\omega t + \delta))} \int_0^t dt' e^{\alpha_2 \cos(\omega t' + \delta)}. \tag{33}$$

The first term of this equation corresponds to a bounded oscillation, but the presence of the integral in the second term makes $x_{\text{cm}}(t)$ unbounded. Due to this term, the soliton will be expelled out of the trap, i.e., $x_{\text{cm}}(t \to \infty) = \pm\infty$. Therefore, the soliton can be localized, by choosing the parameters such that the prefactor of the unbounded term vanishes, namely

$$v_0 = \frac{1}{2}x_0\alpha_2\omega\sin\delta. \tag{34}$$

With this condition, the center of mass of the soliton is given by

$$x_{\text{cm}}(t) = x_0 e^{\frac{\alpha_2}{2}(\cos\delta - \cos(\omega t + \delta))}. \tag{35}$$

This is one of the main conclusions of this paper. It shows that the soliton can be localized at an arbitrary position by oscillating the strength of the trapping potential and the interatomic interaction. Without such oscillations, the soliton will be expelled out of the trap. In fact, this result also holds for any bounded type of oscillations as can be inferred from equation (24). Taking $v_0 + x_0\dot{\gamma}(0) = 0$, this equation gives $x_{\text{cm}}(t) = x_0 e^{\gamma(0)-\gamma(t)}$, which is bounded for any bounded $\gamma(t)$. The different cases of soliton localization and delocalization, described by equation (33), are shown in figures 1 and 2. In figure 1, the soliton is shown to be expelled out of the left (right) side of the trap when $v_0 < x_0\alpha_2\omega\sin(\delta)/2$ ($v_0 > x_0\alpha_2\omega\sin(\delta)/2$), while for $v_0 = x_0\alpha_2\omega\sin(\delta)/2$, the soliton remains localized around its initial position x_0. In figure 2, this is shown with the trajectory of the center of mass of the soliton.

Note that in order to localize the soliton, no condition on ω was required. Therefore, one may argue that by taking ω arbitrarily small, we get a localized soliton in an almost stationary expulsive harmonic trap. This of course contradicts the fact that in an expulsive harmonic trap, solitons are expelled away from the center. However, one should keep in mind that with our special form of $\gamma(t)$, namely equation (30), the strength of the trapping potential will be proportional to ω^2. Therefore, a very small value of ω corresponds to a shallow potential that approaches the homogeneous case for $\omega = 0$. The fact that the strength of the harmonic potential depends on ω leads to conclude that, for deep traps, larger trap oscillations frequency are needed to localize the soliton contrary to the case with shallow traps where the soliton can be localized with smaller trap oscillations frequency.

Taking the time average of the trapping potential $(\omega/2\pi)\int_0^{2\pi/\omega} dt\,(\ddot{\gamma}(t) - \dot{\gamma}(t)^2)x^2/2 = -\alpha_2^2\omega^2 x^2/16$ shows that the soliton spends on the average more time in the expulsive trapping potential. One may thus conclude that after sufficiently long time the soliton will be expelled out of the trap which contradicts our previous localization result. A careful examination of the dynamics shows that this conclusion is incorrect. In spite of the fact that the soliton spends more time in the expulsive trap, the inhomogeneity of the trapping potential can compensate for the time difference. The strength of the trapping potential has in general two periods τ_1 and τ_2, as shown in figure 3. The period τ_1 depends on α_2 and $\tau_2 = 2\pi/\omega$. The strength of the trapping potential is positive for a period of τ_1 and negative for $\tau_2 - \tau_1 > \tau_1$ for all
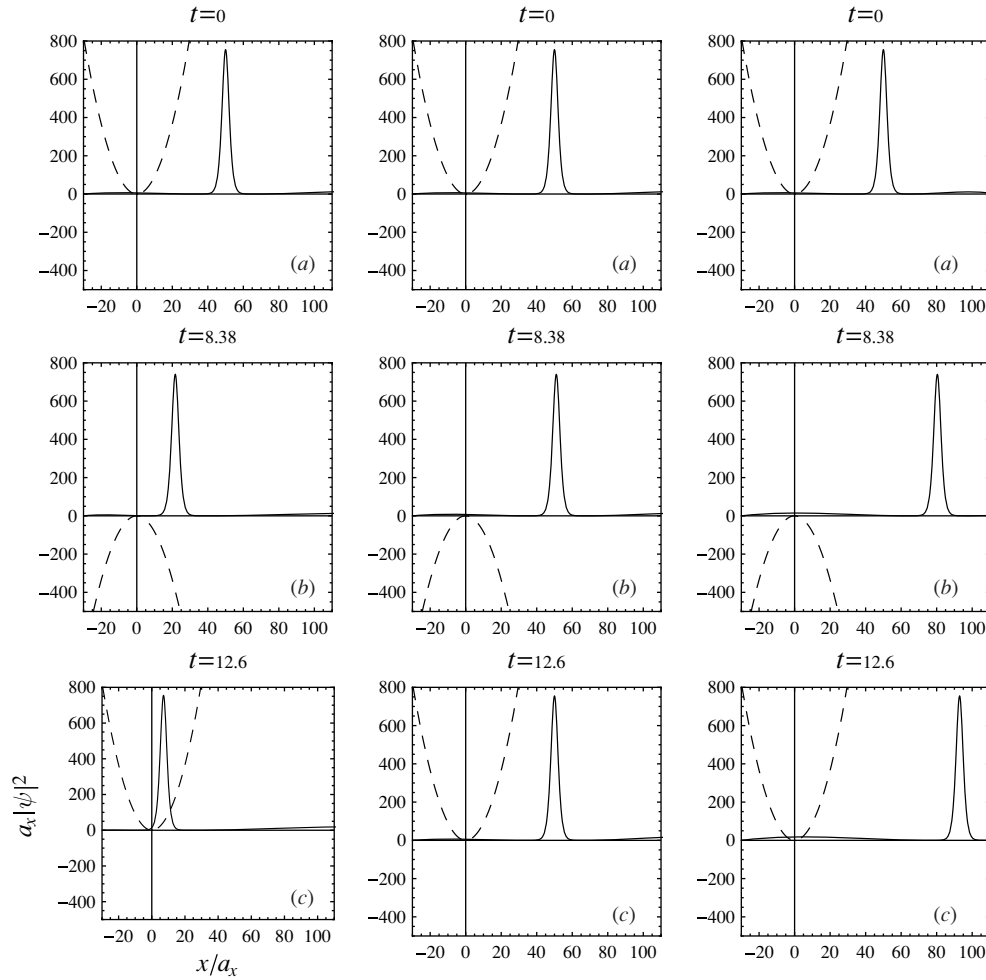
Figure 1. Soliton's density profile (solid curve) and trapping potential (dashed curve). First column of subfigures: $v_0 = 0.8 \times x_0\alpha_2\omega \sin(\delta)/2 = 8.4$. Middle column of subfigures: $v_0 = x_0\alpha_2\omega \sin(\delta)/2 = 10.5$. Last column of subfigures: $v_0 = 1.2 \times x_0\alpha_2\omega \sin(\delta)/2 = 12.6$. For the three cases, we take $\alpha_1 = 1, \alpha_2 = 0.5, \omega = 2, \delta = 1$ and $x_0 = 50$. Time is in units of $1/\omega_x$.

α_2. Assuming the soliton started the motion at $x_0 > 0$ from rest, it will experience at first a harmonic trapping potential for time τ_1 and therefore will move to the left (region of lower potential) for a certain distance. At time τ_1, the trapping potential becomes expulsive for time period $\tau_2 - \tau_1$ and the soliton starts to return back. However, it starts now from a point of lower potential than at x_0 which means that it will experience a weaker trapping potential. Therefore, in order to reach the starting point, x_0, it needs more time compared to the forward part of the motion. If that time matches $\tau_2 - \tau_1$, the soliton returns back to x_0 with zero velocity and the cycle repeats leading to trapping of the soliton, which corresponds to the middle curve of figure 2. On the other hand, if the soliton reaches a point $x > x_0$, it will be eventually expelled out of the right side of the trap corresponding to the upper curve of figure 2, and if it
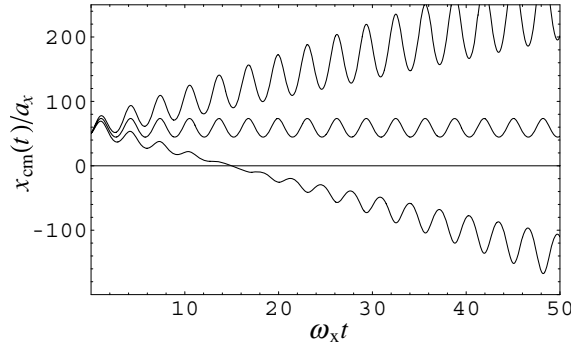
**Figure 2.** Soliton's center-of-mass trajectory for three values of the initial velocity. The upper curve corresponds to $v_0 = 1.2 \times x_0\alpha_2\omega \sin(\delta)/2 = 12.6$, the middle curve corresponds to $v_0 = x_0\alpha_2\omega \sin(\delta)/2 = 10.5$ and the lower curve corresponds to $v_0 = 0.8 \times x_0\alpha_2\omega \sin(\delta)/2 = 8.4$. For the three curves, we take $\alpha_1 = 1$, $\alpha_2 = 0.5$, $\omega = 2$, $\delta = 1$ and $x_0 = 50$.
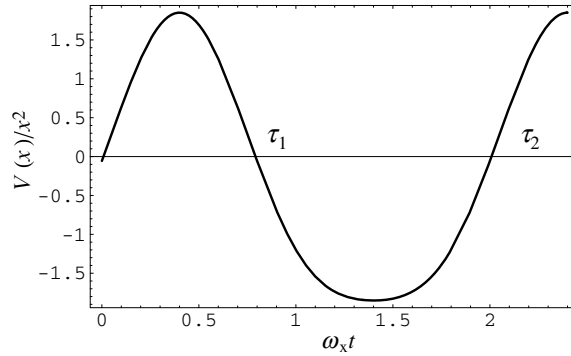
Figure 3. Strength of the trapping potential versus time. The following values were used: $\alpha_1 = 1$, $\alpha_2 = 0.75$, $\omega = \pi$, $\delta = 1.2$.

reaches $x < x_0$, it will be expelled out of the left side of the trap corresponding to the lower curve of figure 2.

To further understand this trapping mechanism, we calculated the trapping potential *felt* by the soliton through its trajectory, namely $V(x_{cm}(t))$, which is plotted in figure 4. In this figure, the dynamics of the soliton is represented by a point moving on the curve with a direction that is indicated on each curve. The center-of-mass motion of figure 2 can be extracted by tracing $x_{cm}(t)$ while the point moves along the potential curves. In figure 4(*a*), the soliton starts at $x_0 = 50$ with initial velocity $v_0 = 1.2\alpha_2 x_0\omega \sin(\delta)/2$. In this case, the soliton gets drifted by time toward larger values of x_{cm} corresponding to the upper curve of figure 1. In figure 4(*c*), the initial velocity is $v_0 = \alpha_2 x_0\omega \sin(\delta)/2$, which results in soliton localization. In this subfigure, the soliton oscillates between $x_{cm} = 50$ and $x_{cm} = 61$ corresponding to the middle curve of figure 2. In figure 4(*e*), the initial velocity is $v_0 = 0.8\alpha_2 x_0\omega \sin(\delta)/2$ leading to a drift toward lower values of x_{cm} corresponding to the lower curve of figure 2. To make an analogy with a classical particle moving in a time-independent potential, we defined $V_{eff}(x_{cm}(t)) = V(x_{cm}(t)) - [V(x_{cm}(\pi/\omega)) - V(x_{cm}(0))][x_{cm}(t) - x_{cm}(0)]/[x_{cm}(\pi/\omega) - x_{cm}(0)]$. In figures 4(*b*), (*d*), (*f*), we plot $V_{eff}(x_{cm})$ that corresponds to figures 4(*a*), (*c*), (*e*), respectively. The
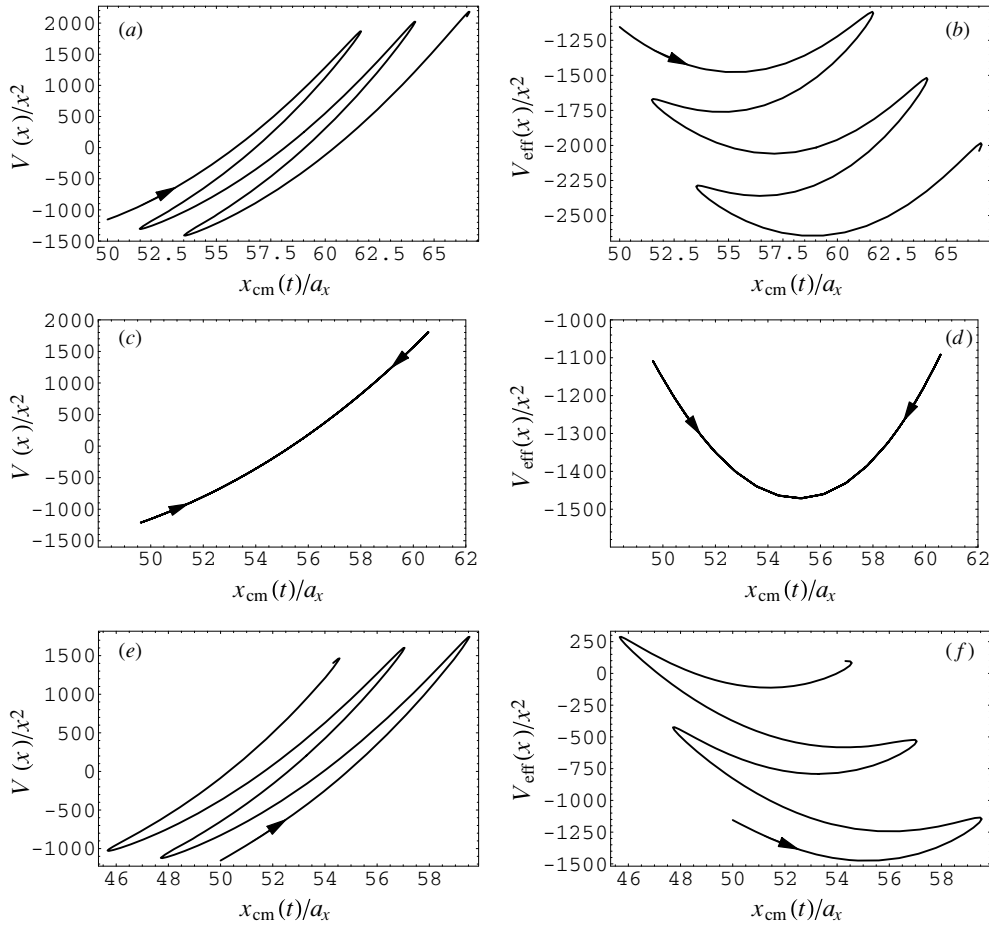
Figure 4. First column: the trapping potential $V(x_{cm}(t))$. Second column: the effective trapping potential $V(x_{cm}(t))$. (*a*) and (*b*) correspond to, $v_0 = 1.2\alpha_2 x_0\omega \sin(\delta)/2$, (*c*) and (*d*) correspond to, $v_0 = \alpha_2 x_0\omega \sin(\delta)/2$, (*e*) and (*f*) correspond to, $v_0 = 0.8\alpha_2 x_0\omega \sin(\delta)/2$. For all curves: $x_0 = 50$, $\alpha_1 = 1$, $\alpha_2 = 0.2$, $\delta = 0.4$, and $\omega = \pi$. The arrows show the direction of the motion of the soliton.

dynamics is now simplified to that of a classical particle oscillating in a *ladder* of parabolic potentials. For the nonlocalized soliton, the potential minimum is shifted by time to the right (figure 4(*b*)) or to the left (figure 4(*f*)). For the localized soliton case, the minimum of the potential is stationary.

3.4. Another family of exact solutions

Using the exact solution found above as a seed solution, the Darboux transformation generates a two-solitons solution. This kind of solution is useful for studying soliton–soliton interactions which is left for future work. Another family of more complicated exact solitonic solutions can be obtained by using a nontrivial seed solution as shown in appendix A. Substituting for $\gamma(t)$ in equation (A.2), we get the second class of exact solutions. This family of solutions is more complicated than the above single-solitonic solution since it involves, in addition to
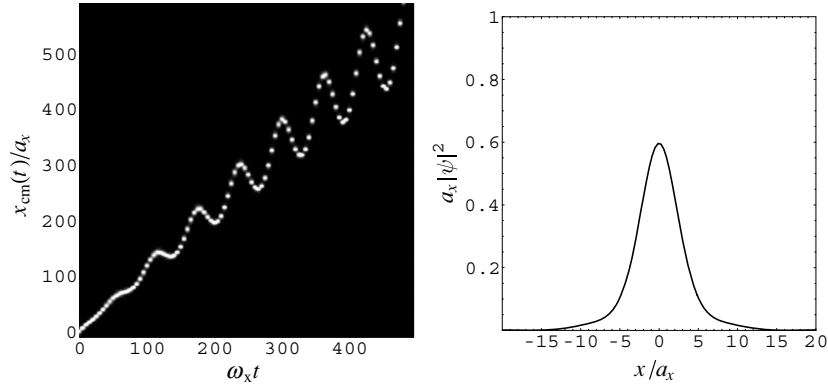
Figure 5. Left: spatiotemporal contour plot of soliton density profile. Right: soliton density profile at $t = 0$. The values of the parameters used in this plot are: $c_1 = -c_2 = 10, c_3 = c_4 = 1, \lambda_{1i} = \lambda_{1r} = 1, A = 2, a = 0.9, k_0 = 5, \lambda = \omega = 1, \delta = 0, \alpha_1 = -6, \alpha_2 = 0.3$. The value of k_0 is the solution of $\alpha = 0$ with respect to k_0.

the single-solitonic solutions, multi-solitonic and solitary wave solutions. Here, we present briefly the main properties of the solutions of this kind. In figure 5, we plot the density of a single-solitonic solution showing that the soliton is being expelled out of the center of the trap. The oscillation in the trajectory of the soliton is due to the oscillating trapping potential. The discontinuous appearing of the soliton is due to the interaction with the background. This trajectory can also be extracted from the general solution, equation (A.2), by considering the term $(\Gamma c_1^2 e^{2\alpha\eta - \sqrt{\bar{\eta}}\Delta_r x} + \Gamma c_2^2 e^{-2\alpha\eta + \sqrt{\bar{\eta}}\Delta_r x})$ in the denominator. At the soliton's density peak this is the dominant term that determines the position of the soliton. Specifically, the position of the peak is given by the condition $2\alpha\eta - \sqrt{\bar{\eta}}\Delta_r x = 0$. Using this condition to plot x versus t in figure 6, we obtain a curve that is identical to the soliton trajectory in figure 5. The mean slope of this curve is proportional to $\alpha/2\Delta_r$. Hence, the rate at which the soliton leaves the center of the trapping potential can be delayed by choosing the parameters and the arbitrary constants such that $\alpha/2\Delta_r$ is small. For the special case of $\alpha = 0$ the center of mass of the soliton will be localized at $x = 0$ indefinitely. In this case, the oscillating trapping potential results only in oscillations in the width and peak density of the soliton. This is also shown in figure 7 where we see a multi-solitonic solution with central soliton being localized at $x = 0$ and off-central ones oscillating around their initial positions. In figure 8, we show that for some values of the parameters the dynamics of the peak soliton density can be so drastic such that the soliton disappears in the background and reappears at regular discrete times.

4. Numerical solution and experimental realization

As we have seen in section 3.3, there is a possibility of localizing the soliton by oscillating the trapping potential and the interatomic interaction in the manner described by equation (31). Such synchronized oscillations may not be possible to realize experimentally. Instead, a setup with an oscillating strength of the trapping potential and constant interatomic interaction may be experimentally more favorable. This situation can be obtained in our case with the condition $\alpha_2 \ll 1$ resulting in the following Gross–Pitaevskii equation:

$$i\frac{\partial\psi(x,t)}{\partial t} = \left[-\frac{\partial^2}{\partial x^2} - \frac{1}{2}\Omega^2\cos(\omega t + \delta)x^2 - a|\psi(x,t)|^2\right]\psi(x,t), \qquad (36)$$
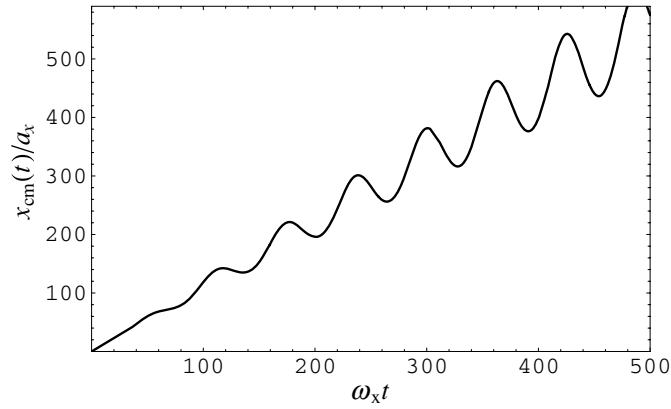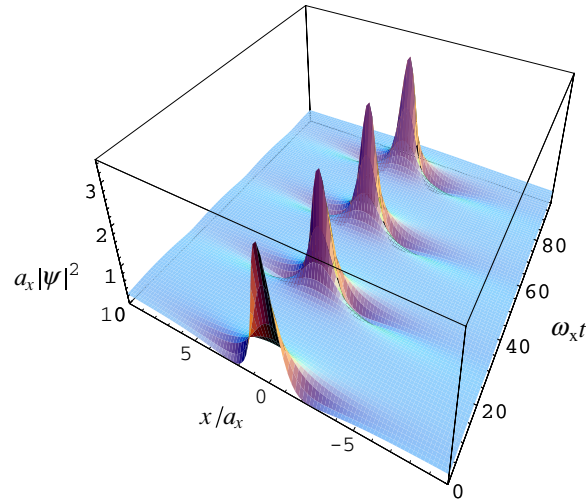
Figure 6. Trajectory of the soliton's peak density. The values of the parameters used here are the same as those of figure 5.
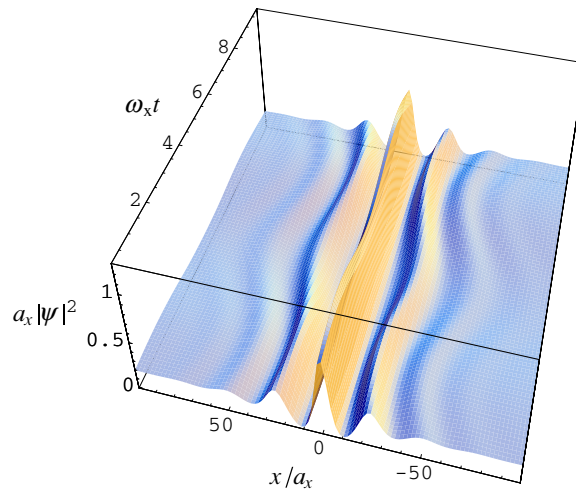

Figure 7. Density profile of a single soliton solution. The values of the parameters used in this plot are: $-c_2 = c_1 = 10, c_3 = c_4 = 1, \lambda_{1i} = \lambda_{1r} = 1, A = 2, a = 0.9, k_0 \sim 5.03, \lambda = \omega = 1, \delta = 0, \alpha_1 = -6, \alpha_2 = 0.3$. The value of k_0 is the solution of $\alpha = 0$ with respect to k_0.

where $\Omega = \omega\sqrt{\alpha_2/2}$ and we have set $\alpha_1 = 0$. We solve this equation numerically using the exact solution of the homogeneous case, namely the solution of equation (36) with $\Omega = 0$, as the initial wavefunction. This can be obtained from equation (22) simply by substituting $\alpha_1 = \alpha_2 = 0$. The soliton's center-of-mass trajectory is extracted from the resulting numerical solution and then plotted versus time as shown in figure 9. The trajectory is shown with the filled circles for $\omega = 2$ and $\Omega = 0.44$ and with the empty circles for $\omega = 2$ and $\Omega = 0.14$. It is clear from this figure that with smaller amplitude of the oscillating trapping potential, the soliton will be localized for longer periods. The solid and dashed curves show the corresponding trajectories in the presence of the oscillating interatomic interaction as described by equation (33). The difference between the solid and filled circle curves shows the important role played by the oscillations in the interatomic interactions in stabilizing the

13

Figure 8. Density profile of a multi-soliton solution. The values of the parameters used in this plot are: $-c_2 = c_1 = 10, c_3 = c_4 = 1, \lambda_{1i} = 0, \lambda_{1r} = 1, A = 2, a = 0.9, k_0 = 0, \lambda = 1, \omega = 0.01, \delta = 0, \alpha_1 = -2, \alpha_2 = 0.3$.
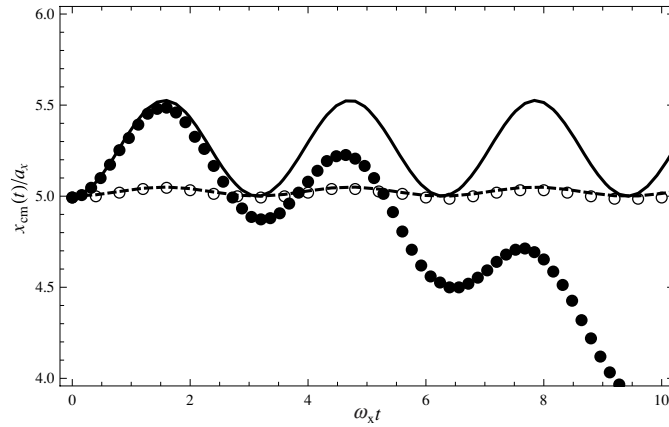
Figure 9. Soliton's center-of-mass trajectory. The solid and dashed curves correspond to the exact formula equation (24). Empty and filled circles correspond to the numerical solution of equation (36). Solid curve and filled circles are obtained with $\Omega = \omega\sqrt{\alpha_2/2} = 0.44\omega_x$ and dashed curve and empty circles are obtained with $\Omega = \omega\sqrt{\alpha_2/2} = 0.14\omega_x$. The rest of parameters used are: $a = 10^{-4}, \delta = v_0 = 0, x_0 = 5, \alpha_1 = 1, N = 4 \times 10^3, \alpha_2 = 0.1$ for the solid curve and $\alpha_2 = 0.01$ for the dashed curve.

soliton. On the other hand, the overlap between the dashed and open circle curves shows that the effect of interatomic interactions is minor for smaller amplitudes of the oscillation in the trapping potential.

The exact center-of-mass dynamics of the solitonic solution of equation (36) is dictated, according to Kohn's theorem [40], by the potential $-\frac{1}{2}\Omega^2 \cos(\omega t + \delta)x^2$ independently from
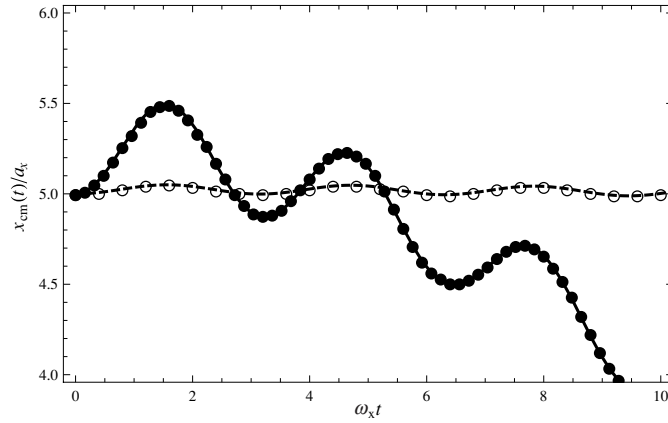
Figure 10. Soliton's center-of-mass trajectory. The solid and dashed curves correspond to the exact formula equation (39). Empty and filled circles correspond to the numerical solution of equation (36). All parameters used are the same as those of figure 9.

the interatomic interaction. Taking advantage of this fact, the equation of motion of the center of mass follows:

$$\ddot{x}_{cm}(t) - \Omega^2 \cos(\omega t + \delta) x_{cm}(t) = 0. \tag{37}$$

The general solution of this equation is a linear combination of the sine and cosine Mathieu functions

$$x_{cm}(t) = c_1 C(0, \alpha_2, (\omega t + \delta)/2) + c_2 S(0, \alpha_2, (\omega t + \delta)/2), \tag{38}$$

where c_1 and c_2 are arbitrary constants. Using the initial conditions $x_{cm}(0) = x_0$ and $\dot{x}_{cm}(0) = 0$, the solution takes the form

$$x_{cm}(t) = \frac{x_0 C(0, \alpha_2, (\omega t + \delta)/2)}{C(0, \alpha_2, \delta/2)}. \tag{39}$$

This solution is plotted in figure 10, where we also plot the result of the numerical solution of equation (36) for the same parameters. The agreement between the numerical and the exact result is evident. The advantage of the exact analytical solution over the numerical one is that we can investigate the long-time dynamics of the soliton. In figure 11, we plot the center of mass of the soliton for a much longer time interval than in figures 9 and 10. This figure shows that the soliton will be trapped over such a large time scale and is oscillating between x_0 and $-x_0$. The frequency of this oscillation is given by the period of the Mathieu function $C(0, \alpha_2, (\omega t + \delta)/2)$. A numerical computation of the first root of this function for different values of α_2 and ω shows that this frequency is proportional to $\alpha_2 \omega$. The constant of proportionality is determined numerically which results in $\omega_P = 0.353\alpha_2\omega$. The fact that the soliton is trapped by the oscillating harmonic potential is a well-established result for such a configuration, known as *Paul trap* [41], which is used to trap cold ions (Hence, ω_P denotes the frequency of the Paul trap.).

To have realistic estimates of the parameters α_1, α_2 and ω, we consider the experiment of Strecker *et al* [5]. In this experiment, solitons were created with a maximum number of $N = 5000^7$ Li atoms per soliton. The solitons' center of mass oscillated with amplitude $\sim 370\ \mu$m and period 310 ms. The strength of the harmonic trapping potential in the radial direction $\omega_\perp = 2\pi \times 800\ \text{rad s}^{-1}$ was much larger than that of the axial direction $\omega_x = 2\pi \times 3$
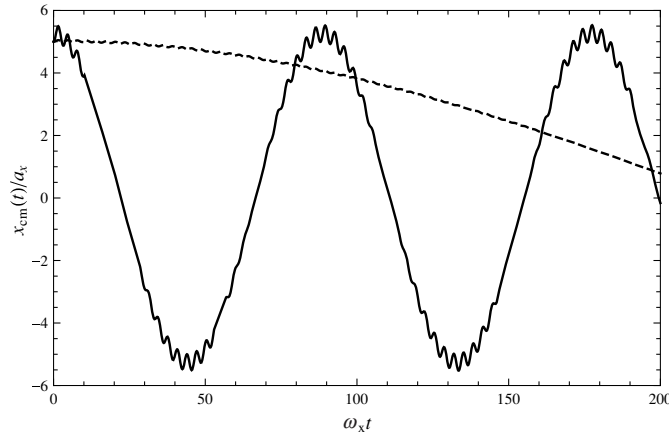
Figure 11. The solid and dashed curves correspond to the exact formula equation (39). The two curves are the same as those of figure 10 but shown here over a larger time interval. Extending the time interval further shows that the dashed curve is also oscillatory.

rad s^{-1}. In this case, the unit of length used in this paper is $a_x \approx 2$ μm and the unit of time is $1/\omega_x \approx 50$ ms. Furthermore, for the ^{7}Li scattering length $a_s \sim 3a_0 = 1.5 \times 10^{-10}$ m, our scaled scattering length is $a = a_s/a_x \simeq 10^{-4}$. In view of these experimental values, figure 9 is explained as follows. The filled circles show a soliton located initially at 10 μm from the trap center. Oscillating the trapping potential with frequency $\Omega = 0.44\omega_x \simeq 2\pi \times 1.3$ rad s^{-1}, the soliton will be drifted a distance of 10 μm from its initial location in a time period of 1.2 s. On the other hand, using a rather more *gentle* oscillation in the trapping potential, namely with $\Omega = 0.14\omega_x \simeq 2\pi \times 0.4$ rad s^{-1}, the soliton will be nearly localized about its initial position over the same time period.

The exact result, equation (33), indicates that the soliton can be trapped at any position and with any trap frequency as long as the trapping potential and the interatomic interaction are oscillating coherently. Furthermore, it shows that the soliton maintains its single-solitonic structure irrespective of the robustness of the trap oscillation. In the present case, where the interatomic interactions oscillation is turned off, the situation may be different. The soliton looses the possibility of indefinite localization and may also loose its single-soliton structure. Solving equation (36) for larger values of Ω and x_0 shows that the soliton will leave its initial position faster and gets fragmented into many solitons that collide and interfere with each other. Therefore, localizing the soliton at larger distances while maintaining its single-solitonic structure requires shallower traps.

5. Conclusions

Using the Darboux transformation method, we derived exact solitonc solutions of a class of Gross–Pitaevskii equations represented by equation (7). The solutions are obtained for a general time-dependent strength of the harmonic trapping potential and a related time-dependent strength of the interatomic interaction. Two classes of exact solitonic solitions were found. The first class represents a single soliton with an arbitrary phase, initial position and initial velocity, as given by equation (22). The second class comprises single, multiple and solitary wave solitonic solutions.

As a specific case, we considered an oscillating trapping potential and interatomic interaction, as given by equations (30) and (31). We found that the soliton can be localized at an arbitrary position and for any amplitude and frequency of the oscillating trapping potential. This localization is possible in spite of the asymmetric oscillation where the trapping potential spends more time being expulsive. In such a case, one expects that by time the soliton will be expelled out of the trap. It turns out, however, that the inhomogeneity in the trapping potential has a balancing effect such that it becomes possible to localize the soliton indefinitely. As a consequence of the previously mentioned approximate nature of the Gross–Pitaevskii equation, the fact that our solutions have a δ-function center of mass is also approximate [42]. For finite number of atoms, the center of mass spreads which may lead to the delocalization of the soliton. For small variations in the center of mass, the soliton is expected to remain localized, but when the center of mass spreading is larger than the amplitude of the soliton oscillation around its equilibrium point, we expect that localization disappears completely.

To discuss the experimental realization, we considered a simpler situation with an oscillating trapping potential and constant interatomic interaction, as described by equation (36). The numerical solution of this equation showed that soliton localization is possible but for a finite time that can be controlled by the frequency and amplitude of the trapping potential oscillation. It is shown that for the ^{7}Li experiment of Strecker *et al* [5], the soliton can be localized for a time long enough to be observed. With smaller frequency and amplitude, the localization time becomes even larger.

The Gross–Pitaevskii equation provides an accurate description of the dynamics of solitons as long as finite-temperature effects are suppressed and atom losses are negligible [22]. At finite temperatures and with atom losses, the soliton broadens and starts to loose it particle-like behavior. When exposed to oscillations in the trapping potential, the soliton will, in this case, be fragmented and soliton localization may not hold.

Using the localization mechanism, solitons can be prepared in arbitrary initial conditions. This may be useful for studying soliton–soliton collisions or the interaction of solitons with potentials. For instance, the shallow oscillating trap can be turned on immediately after the solitons were created which leads to localizing the soliton at a certain position. Then by switching on and off the oscillating trap the soliton can be moved from one point to the other.

Appendix A. Exact solutions using a nonzero seed

A nontrivial seed solution can be easily obtained by substituting in equation (7) $\psi(x,t) = \exp(h_1(t) + ih_2(x,t))$, where $h_1(t)$ and $h_2(x,t)$ are real functions

$$
\psi_0(x,t) = A \exp\left[\frac{\dot{\gamma}(t)}{2} - \frac{i}{4}\left(4aA^2 - 4e^{\dot{\gamma}(t)}xk_0 - 2k_0{}^2 \right.\right.
$$
$$
\left.\left. + 4\int e^{2\dot{\gamma}(t)}dt(-2aA^2 + k_0{}^2) + x^2\ddot{\gamma}(t) \right)\right]. \tag{A.1}
$$

Here A and k_0 are arbitrary constants.

Solving the linear system (4) and (5) using the seed solution, equation (A.1), and then substituting for $\psi_0(x,t)$, $\psi_1(x,t)$ and $\phi_1(x,t)$ in the last equation, we obtain the following

new exact solution of equation (7):

$$\psi(x,t) = \dot{\eta}^{1/4}e^{-i\ddot{\eta}x^2/8\dot{\eta}}\left\{ Ae^{q_1} \right.$$
$$+ 4\lambda_{1r}e^{i\theta_4+q_2}(2ic_3A\sqrt{a}e^{2\alpha\eta} + c_4q_3e^{-2i\theta_1+\Delta_r\sqrt{\dot{\eta}}x})(c_3q_3^*e^{2\alpha\eta} - 2iA\sqrt{a}c_4e^{-i\theta_3+\Delta_r\sqrt{\dot{\eta}}x})$$
$$\left/ \left[c_1^2\Gamma e^{2\alpha\eta-\Delta_r\sqrt{\dot{\eta}}x} + c_2^2\Gamma e^{-2\alpha\eta+\Delta_r\sqrt{\dot{\eta}}x} - 4Ac_1c_2\sqrt{a}[(2\lambda_{1r} - \Delta_r)(\cos 2\theta_1 + \cos\theta_3) \right.\right.$$
$$\left.\left. + (\Delta_i - 2\lambda_{1r})(\sin 2\theta_1 + \sin\theta_3) + (\sin 2\theta_1 + \sin\theta_3)k_0) \right] \right\}, \tag{A.2}$$

where

$$q_1 = i[2A^2a(2\eta - 1) + k_0(k_0(1 - 2\eta) + 2\sqrt{\dot{\eta}})x]/2,$$

$$q_2 = -2\alpha\eta - \Delta\sqrt{\dot{\eta}}x,$$

$$q_3 = \Delta_i + k_0 + i(\Delta_r + 2i\lambda_{1i} - 2\lambda_{1r}),$$

$$\theta_1 = \Delta_r\lambda_{1r}\eta - ((2\lambda_{1i} + k_0) - \sqrt{\dot{\eta}})\Delta_i/2,$$

$$\theta_2 = \left(k_0^2(1 - 2\eta) - 4\Delta_r\lambda_{1r}\eta\right)/4 + 2A^2a(1 - 2\eta)$$
$$+ 2\Delta_i(2\lambda_{1i}\eta - \sqrt{\dot{\eta}}x) + 2k_0(\Delta_i\eta + \sqrt{\dot{\eta}}x),$$

$$\theta_3 = (2\Delta_i\lambda_{1i} - 2\Delta_r\lambda_{1r} + \Delta_ik_0)\eta - \sqrt{\dot{\eta}}\Delta_ix,$$

$$\theta_4 = k_0\sqrt{\dot{\eta}}x + \left(2A^2a - k_0^2\right)(2\eta - 1)/2,$$

$$\Gamma = (\Delta_i - 2\lambda_{1i})^2 + (\Delta_r - 2\lambda_{1r})^2 + 4A^2a + k_0(2\Delta_i - 4\lambda_{1i} + k_0),$$

$$\alpha = \Delta_r\lambda_{1i} + \Delta_i\lambda_{1r} + \Delta_rk_0/2,$$

$$\Delta_r = \text{Re}[\sqrt{(2\lambda_1 - ik_0)^2 - 4A^2a}],$$

$$\Delta_i = \text{Im}[\sqrt{(2\lambda_1 - ik_0)^2 - 4A^2a}],$$

$$\gamma = \Delta_i + k_0 + i(\Delta_r + 2i\lambda_{1i} - 2\lambda_{1r}),$$

$$\eta(t) = \int e^{2\dot{\gamma}(t)}dt,$$

and c_1 and c_2 are arbitrary constants. It should be noted that this is an exact solution of equation (7) for any $\gamma(t)$.

There are five arbitrary parameters in the general solution, namely k_0, A, λ_1, c_1 and c_2. The first three parameters control the phase and amplitude of the seed solution which is part of the general solution. The last two parameters control the amplitude and phase of the general solution. The solitonic solutions represented by equation (A.2) are nonsingular for all x and t since the denominator of this equation does not vanish. This can be easily deduced from equation (20) where we see that the denominator of equation (A.2) is merely the amplitude of ϕ_1 and ψ_1 that vanishes only if we have the trivial solution with $c_1 = c_2 = 0$.

References

[1] Burger S, Bongs K, Dettmer S, Ertmer W, Sengstock K, Sanpera A, Shlyapnikov G V and Lewenstein M 1999 *Phys. Rev. Lett.* **83** 5198
[2] Denschlag J *et al* 2000 *Science* **287** 97
[3] Anderson B P, Haljan P C, Regal C A, Feder D L, Collins L A, Clark C W and Cornell E A 2001 *Phys. Rev. Lett.* **86** 2926
[4] Khaykovich L, Schreck F, Ferrari G, Bourde T, Cubizolles J, Carr L D, Castin Y and Salomon C 2002 *Science* **296** 1290
[5] Strecker K E, Partridge G B, Truscott A G and Hulet R G 2002 *Nature* **417** 150
[6] Eiermann B, Anker Th, Albiez M, Taglieber M, Treutlein P, Marzlin K-P and Oberthaler M K 2004 *Phys. Rev. Lett.* **92** 230401
[7] Perez-Garcia V M, Michinel H and Herrero H 1998 *Phys. Rev. A* **57** 3837
[8] Busch Th and Anglin J R 2000 *Phys. Rev. Lett.* **84** 2298
[9] Al Khawaja U, Stoof H T C, Hulet R G, Strecker K E and Partridge G B 2002 *Phys. Rev. Lett.* **89** 200404
[10] Carr L D and Castin Y 2002 *Phys. Rev. A* **66** 063602
[11] Carr L D and Brand J 2004 *Phys. Rev. Lett.* **92** 040401
[12] Kasamatsu K and Tsubota M 2004 *Phys. Rev. Lett.* **93** 100402
[13] Salasnich L 2004 *Phys. Rev. A* **70** 053617
[14] Abdullaev F K, Gammal A, Kamchatnov A and Tomio L 2005 *Int. J. Mod. Phys.* B **19** 3415
[15] Salasnich L, Parola A and Reatto L 2003 *Phys. Rev. Lett.* **91** 080405
[16] Zabusky N J and Zabusky N J 1965 *Phys. Rev. Lett.* **15** 240
[17] Hasegawa A and Tappert F D 1973 *Appl. Phys. Lett.* **23** 171
[18] Chen H H and Liu C S 1976 *Phys. Rev. Lett.* **37** 693
    Chen H H and Liu C S 1978 *Phys. Fluids* **21** 377
[19] Konotop V V 1993 *Phys. Rev. E* **47** 1423
[20] Tsuchiya S, Dalfovo F and Pitaevskii L P 2008 *Phys. Rev. A* **77** 045601
[21] Serkin V N, Hasegawa A and Belyaeva T L 2007 *Phys. Rev. Lett.* **98** 074102
[22] See for instance, Pethick C J and Smith H 2001 *Bose–Einstein Condensation in Dilute Gases* (Cambridge: Cambridge University Press)
[23] Saito H and Ueda M 2003 *Phys. Rev. Lett.* **90** 040403
[24] Gross E P 1961 *Nuovo Cimento* **20** 454
[25] Pitaevskii L P 1961 *Zh. Eksper. Teor. Fiz.* **40** 646
[26] Weiss C and Castin Y 2009 *Phys. Rev. Lett.* **102** 010403
[27] Liu W-M, Wu B and Niu Q 2000 *Phys. Rev. Lett.* **84** 2294
[28] Serkin V N and Hasegawa A 2002 *IEEE J. Sel. Top. Quantum Electron.* **8** 418
[29] Ieda J, Miyakawa T and Wadati M 2004 *Phys. Rev. Lett.* **93** 194102
[30] Liang Z X, Zhang Z D and Liu W M 2005 *Phys. Rev. Lett.* **94** 050402
[31] Li L, Li Z, Malomed B A, Mihalache D and Liu W M 2005 *Phys. Rev. A* **72** 033611
[32] Atre R, Panigrahi P K and Agarwal G S 2006 *Phys. Rev. E* **73** 056611
[33] Al Khawaja U 2007 *Phys. Rev. E* **75** 066607
[34] Kumar V R, Radha R and Panigrahi P K 2008 *Phys. Rev. A* **77** 023611
[35] Gordon J P 1983 *Opt. Lett.* **8** 596
[36] Matveev V B and Salle M A 1991 *Dardoux Transformations and Solitons (Springer Series in Nonlinear Dynamics)* (Berlin: Springer)
[37] Carr L D, Clark C W and Reinhardt W P 2000 *Phys. Rev. A* **62** 063610
    Carr L D, Clark C W and Reinhardt W P 2000 *Phys. Rev. A* **62** 063611
[38] Al Khawaja U 2006 *J. Phys. A: Math. Gen.* **39** 9679
[39] Zakharov V E and Shabat A B 1974 *Funct. Anal. Appl.* **8** 226
    Zakharov V E and Shabat A B 1980 *Funct. Anal. Appl.* **13** 166
[40] Kohn W 1961 *Phys. Rev.* **123** 1242
[41] See, for instance, Paul W 1998 *Rev. Mod. Phys.* **62** 531
[42] Calogero F and Degasperis A 1975 *Phys. Rev. A* **11** 265